Peering towards Cosmic Dawn
Proceedings IAU Symposium No. 333, 2018
Vibor Jelić & Thijs van der Hulst, eds.

DOI: 00.0000/X000000000000000X

Evolution of the Quasar Luminosity Function: Implications for EoR-21cm

Girish Kulkarni[1,2], Tirthankar Roy Choudhury[3], Ewald Puchwein[1] and Martin G. Haehnelt[1]

[1]Institute of Astronomy and Kavli Institute of Cosmology, University of Cambridge, Madingley Road, Cambridge CB3 0HA, UK
[2]email: kulkarni@ast.cam.ac.uk
[2]National Centre for Radio Astrophysics, Tata Institute of Fundamental Research, Post Bag 3, Ganeshkhind, Pune 411007, India

Abstract. We present predictions for the spatial distribution of 21 cm brightness temperature fluctuations from high-dynamic-range simulations for AGN-dominated reionization histories that have been tested against available Lyα and CMB data. We model AGN by extrapolating the observed M_{bh}–σ relation to high redshifts and assign them ionizing emissivities consistent with recent UV luminosity function measurements. AGN-dominated reionization histories increase the variance of the 21 cm emission by a factor of up to ten compared to similar reionization histories dominated by faint galaxies, to values close to 100 mK^2 at scales accessible to experiments ($k \lesssim 1$ cMpc^{-1}h). This is lower than the sensitivity reached by ongoing experiments by only a factor of about two or less. AGN dominated reionization should be easily detectable by LOFAR (and later HERA and SKA1) at their design sensitivity.

Keywords. dark ages, reionization, first stars – galaxies: active – galaxies: high-redshift – galaxies: quasars – intergalactic medium

---

Although hydrogen reionization is generally thought to be caused by Lyman continuum photons produced by young stars in low-mass galaxies (Mitra et al. 2015), the idea that active galactic nuclei (AGN) could have been the dominant source of ionizing radiation during the epoch of reionization has recently gained traction again (Giallongo et al. 2015; Madau & Haardt 2015). This is due to a number of recent developments, most prominent among which is the claimed discovery of 19 low-luminosity ($M_{1450} > -22.6$) AGN between redshifts $z = 4.1$ and 6.3 by Giallongo et al. (2015) using a novel X-ray/NIR selection criterion, which may suggest that the faint end of the quasar UV luminosity function is steeper at these redshifts than previously thought (Hopkins et al. 2007; Haardt & Madau 2012). Chardin et al. (2017) demonstrated that the large scatter observed in Lyα opacity between different sightlines close to redshift $z = 6$ (Becker et al. 2015) arises naturally if there is a significant contribution ($\gtrsim 50\%$) of AGN to the ionising emissivity at these redshifts. The uncertainty in the Lyman-continuum escape fraction of high-redshift galaxies (e.g., Japelj et al. 2017; Micheva et al. 2017) further bolsters the possibility that AGN may have played a non-trivial role in hydrogen reionization. It is thus pertinent to ask what a significant contribution of AGN to the ionising emissivity during reionization implies for the search for the 21 cm signal from the epoch of reionization. Here we present predictions for the 21 cm power spectrum from redshifts $z = 7$–10 in models of reionization in which the hydrogen-ionizing emissivity is dominated by AGN and compare them to galaxy-dominated models.

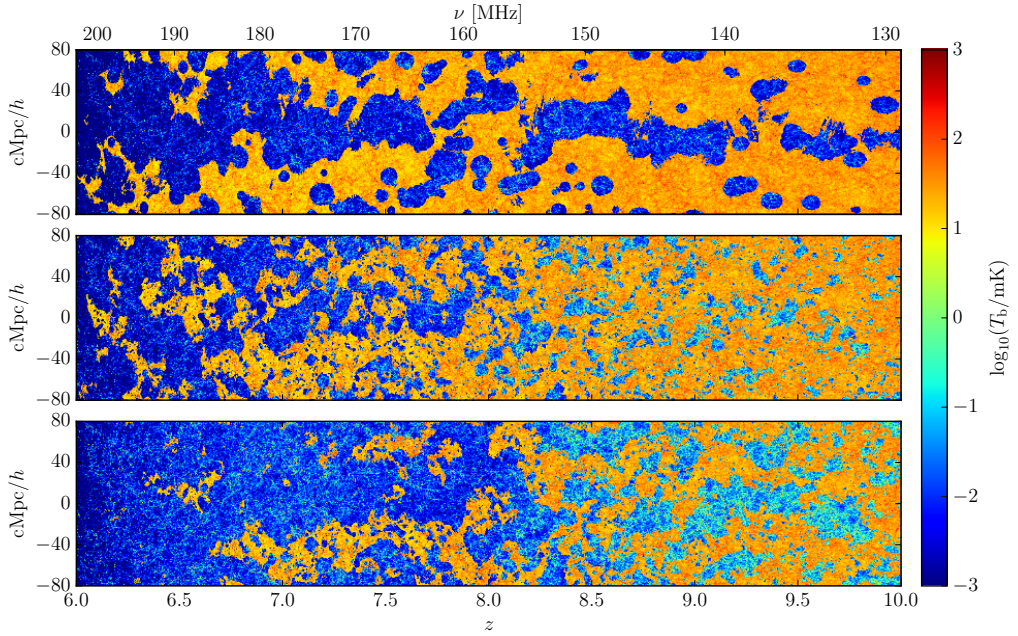

Figure 1. Evolution of the 21 cm brightness temperature distribution from redshift $z = 10$ to 6 in the AGN-dominated Very Late model (top panel), the galaxies-dominated Very Late model (middle panel), and the galaxies-dominated Late/Default model. (Figure 2 from "Large 21-cm signals from AGN-dominated reionization", Kulkarni et al., Monthly Notices of the Royal Astronomical Society, 2017 469 4283.)

1. Methods

Our 21 cm predictions are based on cosmological hydrodynamical simulations that are part of the Sherwood simulation suite (nottingham.ac.uk/astronomy/sherwood; Bolton et al. 2017). Sources of ionizing radiation are placed in haloes identified in the simulation, and an ionization field is obtained using the well-known excursion set approach. This ionization field is then calibrated to the Very Late reionization model of Kulkarni et al. (2016). In this manner, our models self-consistently predict, at high resolution, the large-scale distribution of neutral hydrogen for reionization histories consistent with constraints during the late stages of reionization. We assume that in high-mass haloes that host luminous AGN, the total number of photons $N_\gamma(M)$ produced in a halo of mass M is proportional to the black hole mass $M_{\rm bh}$. In order to estimate the mass of black holes in these haloes, we follow the approach of Kulkarni & Loeb (2012) and employ the $M_{\rm bh}$–σ relation (cf. Mao & Kim 2016) to obtain

$$\frac{M_{\rm bh}}{10^8 {\rm M}_\odot} = 0.12 \left(\frac{M_{\rm halo}}{10^{12} {\rm M}_\odot} \right)^{1.6} \left[\frac{\Omega_m}{\Omega_m^z} \frac{\Delta_c}{18\pi^2} \right]^{0.8} (1+z)^{2.4}. \quad (1.1)$$

for halos above a circular velocity threshold (Kulkarni et al. 2017). In our fiducial AGN-dominated model, we fix the value of the threshold mass M_q to that corresponding to a circular velocity of $v_c = 175$ km/s (Merloni & Heinz 2008; Kelly & Merloni 2012). Our AGN emissivity evolution agrees closely the fit by Madau & Haardt (2015) to the integrated 1 Ry emissivity from AGN down to UV luminosities of $0.01L_*$ (Giallongo et al. 2015).

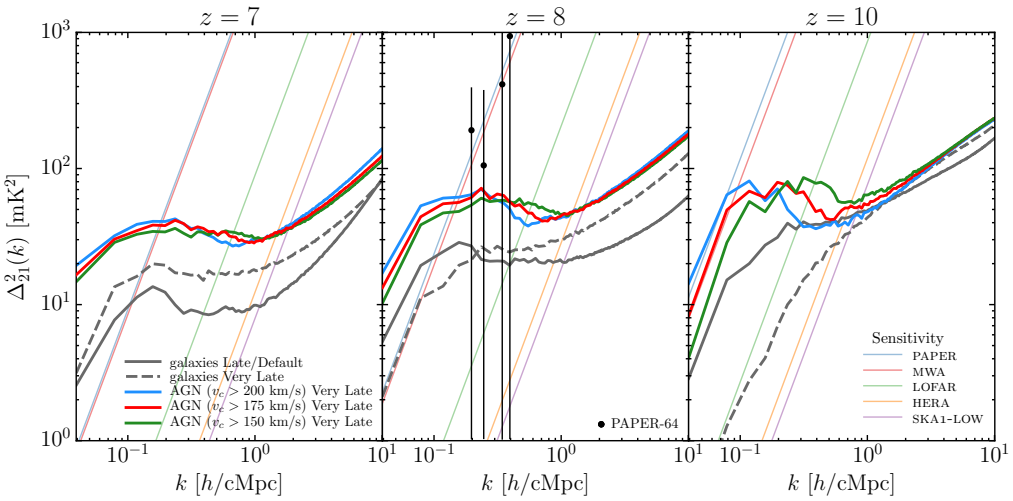

Figure 2. Red curves show the 21 cm power spectra from our fiducial AGN-dominated model, which assumes that AGN are hosted by haloes with circular velocities greater than $v_c = 175$ km/s. Green and blue curves show the power spectra in models where this threshold is changed to 150 km/s and 200 km/s, respectively. Power spectra from the galaxy-dominated Late/Default model of Kulkarni et al. (2016) are shown by the solid grey curves. Dashed grey curves show power spectra from a galaxy-dominated Very Late model, also from Kulkarni et al. (2016). Thin coloured diagonal lines indicate experimental sensitivites. Data points are the measurements from the 64-element deployment of PAPER at $z = 8.4$ (Ali et al. 2015). (Figure 3 from "Large 21-cm signals from AGN-dominated reionization", Kulkarni et al., Monthly Notices of the Royal Astronomical Society, 2017 469 4283.)

2. Results

The top panel of Figure 1 shows the evolution of the 21 cm brightness temperature from redshift $z = 10$ to 6 in our fiducial $v_c > 175$ km/s AGN-dominated model. For comparison, the middle panel of Figure 1 shows the evolution of the 21 cm brightness in the galaxies-dominated Very Late model considered by Kulkarni et al. (2016). The reionization history of this model is identical to that of our AGN-dominated model, so the differences in the brightness distribution between the top and middle panels of Figure 1 arise solely due to differences in the source model. The AGN-dominated model has fewer, larger, and more clustered ionized regions than the galaxies-dominated model (cf. McQuinn et al. 2007). Figure 1 also shows the galaxies-dominated Late/Default model of Kulkarni et al. (2016) in the bottom panel. The source model as well as the reionization history are now different from our AGN-dominated model. This is reflected in a strikingly different morphology of 21-cm-bright regions.

Figure 2 shows the 21 cm power spectra at redshifts $z = 7$, 8, and 10 in its left, middle, and right panels, respectively. The red curve in all panels shows the 21 cm power spectrum in our fiducial AGN-dominated model, in which AGN are hosted by haloes with $v_c > 175$ km/s. The power spectrum is characterised by a bump at large scales and an increase towards the smallest scales. At redshifts $z = 7$–10 shown, the bump occurs at $k \sim 0.2$ cMpc^{-1}h and has an amplitude of approximately $\Delta^2_{21} \sim 40$–70 mK^2. This is significantly higher than in the galaxies-dominated models. (Note that $k = 0.2$ cMpc^{-1}h corresponds to a length scale of 30 h^{-1}cMpc, which is well-sampled in our simulation cube, which is 160 h^{-1}cMpc on each side.) The thin diagonal lines in each panel of Figure 2 show sensitivities set by thermal noise for five ongoing and upcoming 21 cm

experiments. SKA1-LOW and HERA have the highest sensitivities primarily due to large number of antenna elements. In the galaxies-dominated Late/Default model, at $z = 10$ (129 MHz), the signal to noise ratio (SNR) is ~ 100 for these two experiments at $k \sim 0.1$ cMpc^{-1}h. This is enhanced by a further factor of ~ 2 in the AGN-dominated model. The 21 cm signal will be significantly easier to detect if reionization is AGN-dominated. Conversely, these could become the first non-trivial models of reionization to be ruled out by 21 cm experiments, thereby constraining the contribution of AGN to reionization and thus complementing infrared surveys.

3. Conclusions

We have presented predictions of the spatial distribution of the 21 cm brightness temperature fluctuations from AGN-dominated models of reionization using high-dynamic-range cosmological hydrodynamical simulations. Our main conclusion is that AGN-dominated reionization histories increase the large-scale 21 cm power by factors of up to ten relative to galaxy-dominated reionization histories. Conventional models typically predict values of 10–20 mK^2 for the variance of the 21 cm brightness temperature at redshifts $z = 7$–10 at scales accessible to ongoing and upcoming experiments ($k \lesssim 1$ cMpc^{-1}h), but AGN-dominated models can increase this variance to values close to 100 mK^2. This bodes well for experiments that seek to detect this feature, and the predicted signal is lower than the sensitivity claimed to have been already reached by ongoing experiments by only a factor of about two or less. Our models for the reionization history and Lyman continuum emissivity of AGN suggest that these models could become the first non-trivial hydrogen reionization scenarios to be ruled out by experiments, thereby complementing infrared searches for high-z AGN, and constraining the contribution of AGN to reionization.

References

Ali Z. S., et al., 2015, ApJ, 809, 61
Becker G. D., Bolton J. S., Madau P., Pettini M., Ryan-Weber E. V., Venemans B. P., 2015, MNRAS, 447, 3402
Bolton J. S., Puchwein E., Sijacki D., Haehnelt M. G., Kim T.-S., Meiksin A., Regan J. A., Viel M., 2017, MNRAS, 464, 897
Chardin J., Puchwein E., Haehnelt M. G., 2017, MNRAS, 465, 3429
Giallongo E., et al., 2015, A&A, 578, A83
Haardt F., Madau P., 2012, ApJ, 746, 125
Hopkins P. F., Richards G. T., Hernquist L., 2007, ApJ, 654, 731
Japelj J., et al., 2017, MNRAS, 468, 389
Kelly B. C., Merloni A., 2012, Advances in Astronomy, 2012, 970858
Kulkarni G., Loeb A., 2012, MNRAS, 422, 1306
Kulkarni G., Choudhury T. R., Puchwein E., Haehnelt M. G., 2016, MNRAS,
Kulkarni G., Choudhury T. R., Puchwein E., Haehnelt M. G., 2017, MNRAS, 469, 4283
Madau P., Haardt F., 2015, ApJ, 813, L8
Mao J., Kim M., 2016, ApJ, 828, 96
McQuinn M., Lidz A., Zahn O., Dutta S., Hernquist L., Zaldarriaga M., 2007, MNRAS, 377, 1043
Merloni A., Heinz S., 2008, MNRAS, 388, 1011
Micheva G., Iwata I., Inoue A. K., Matsuda Y., Yamada T., Hayashino T., 2017, MNRAS, 465, 316
Mitra S., Choudhury T. R., Ferrara A., 2015, MNRAS, 454, L76